AIP | Applied Physics Letters

Ambipolar inverters using SnO thin-film transistors with balanced electron and hole mobilities

Ling Yan Liang, Hong Tao Cao, Xiao Bo Chen, Zhi Min Liu, Fei Zhuge et al.

Citation: Appl. Phys. Lett. **100**, 263502 (2012); doi: 10.1063/1.4731271
View online: http://dx.doi.org/10.1063/1.4731271
View Table of Contents: http://apl.aip.org/resource/1/APPLAB/v100/i26
Published by the American Institute of Physics.

Related Articles

Telecommunications-band heralded single photons from a silicon nanophotonic chip
Appl. Phys. Lett. 100, 261104 (2012)

Homo-junction ferroelectric field-effect-transistor memory device using solution-processed lithium-doped zinc oxide thin films
Appl. Phys. Lett. 100, 253507 (2012)

Improved sensing performance of polycrystalline-silicon based dual-gate ion-sensitive field-effect transistors using high-k stacking engineered sensing membrane
Appl. Phys. Lett. 100, 253703 (2012)

Multiple silicon nanowire complementary tunnel transistors for ultralow-power flexible logic applications
Appl. Phys. Lett. 100, 253506 (2012)

Influence of channel material properties on performance of nanowire transistors
J. Appl. Phys. 111, 124509 (2012)

Additional information on Appl. Phys. Lett.

Journal Homepage: http://apl.aip.org/
Journal Information: http://apl.aip.org/about/about_the_journal
Top downloads: http://apl.aip.org/features/most_downloaded
Information for Authors: http://apl.aip.org/authors

ADVERTISEMENT

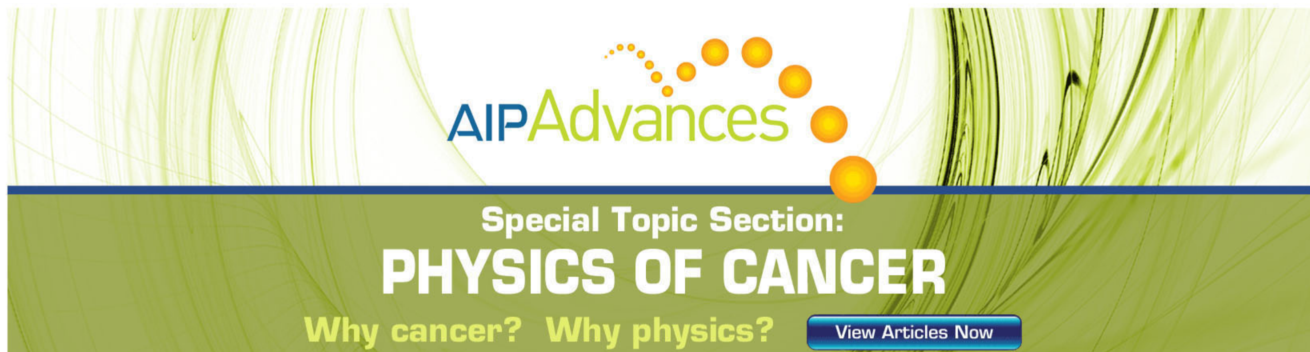

Downloaded 26 Jun 2012 to 210.72.19.250. Redistribution subject to AIP license or copyright; see http://apl.aip.org/about/rights_and_permissions

Ambipolar inverters using SnO thin-film transistors with balanced electron and hole mobilities

Ling Yan Liang,[1] Hong Tao Cao,[1,a)] Xiao Bo Chen,[1] Zhi Min Liu,[1] Fei Zhuge,[1] Hao Luo,[1] Jun Li,[1] Yi Cheng Lu,[2] and Wei Lu[3]
[1]*Division of Functional Materials and Nano Devices, Ningbo Institute of Materials Technology and Engineering (NIMTE), Chinese Academy of Sciences (CAS), Ningbo 315201, People's Republic of China*
[2]*Department of Electrical and Computer Engineering, Rutgers University, Piscataway, New Jersey 08854, USA*
[3]*Department of Electrical Engineering and Computer Science, University of Michigan, Michigan 48109, USA*

(Received 27 March 2012; accepted 11 June 2012; published online 26 June 2012)

Ambipolar thin film transistors have attracted increasing research interests due to their promising applications in complementary logic circuits and the dissipative charge transporting devices. Here, we report the fabrication of an ambipolar transistor using tin mono-oxide (SnO) as a channel, which possesses balanced electron and hole field-effect mobilities. A complementary metal oxide semiconductor-like inverter using the SnO dual operation transistors is demonstrated with a maximum gain up to 30 and long-term air stability. Such logic device configuration would simplify the circuit design and fabrication process, offering more opportunities for designing and constructing oxide-based logic circuits. © *2012 American Institute of Physics*.
[http://dx.doi.org/10.1063/1.4731271]

Oxide thin-film transistor (TFT)-based electronic components such as inverters and logic circuits are attractive due to their low-cost, low-temperature fabrication, and ease of large-area processability.[1–4] In addition to exploring high performance unipolar oxide TFTs, ambipolar thin film transistors based on both *p*-type and *n*-type channels in one device with thereby simplified circuit design and fabrication processes (no separate patterning or/and doping steps needed), are gaining ever-increasing attention as an alternative approach to realizing integrated circuits like radio-frequency identification (RFID) tags or drivers for display applications.[5,6] However, oxide semiconductors with excellent performance are almost *n*-type and there are few *p*-type oxides suitable for electronic devices, because hole transport is restricted in oxide semiconductors due to their deep valence band maximum (VBM) composed of 2p orbitals of oxygen ions with strong directivity and large electronegativity.[7] Therefore, most of the complementary metal oxide semiconductor (CMOS)-like inverters were presented as hybrid circuits combined with *p*-channel organic TFTs.[8–10]

Recently, tin monoxide (SnO) with litharge-type layered structure has been confirmed to be a appreciate *p*-type semiconductor because of its Sn 5s nature near the VBM.[11–13] We already reported that SnO exhibited a reasonably high hole Hall mobility of $\sim$3.9 $cm^2 V^{-1} s^{-1}$ at room temperature,[14] and also fabricated SnO-based *p*-channel TFTs.[14,15] Subsequently, several groups have reported polycrystalline SnO TFTs as well as inverters composed of a *p*-channel SnO_x TFT and a *n*-channel TFT based on other *n*-type oxides.[2,16–18] Moreover, our previous studies have revealed a fundamental but attractive property of SnO, i.e., it has a large direct optical band-gap of 2.68–2.78 eV despite a small fundamental band-gap of $\sim$0.5 eV.[15,19] In principle, the wide optical band-gap of SnO preserves rather high transparency in the visible region, while the small band-gap favors the ambipolar behavior.[20] Very recently, a CMOS-like inverter based on ambipolar SnO TFTs has been demonstrated on SiO_2/Si.[21] However, the inverter presented very low voltage gains ($\leq$2.5) as well as the asymmetric characteristics in the first and third quadrant caused by the tremendously unbalanced hole and electron mobilities of the TFTs. For constructing high-performance inverters based on ambipolar transistors, the key point is to balance both the injection and the transport of holes and electrons.[22] In this letter, we fabricated SnO ambipolar TFTs with balanced hole and electron saturation field-effect mobilities through efforts in the two above-mentioned aspects. Subsequently, an ambipolar inverter working well in both the first and third quadrants is realized with output voltage gains over 30 by integrating two identical ambipolar SnO TFTs, behaving as a valuable building block of oxide logic circuits. Moreover, the inverter exhibits excellent environmental stability, a prerequisite for the future ubiquitous electronics. These results also manifest that, a simple route in realizing oxide-based ambipolar TFTs and CMOS-like inverters, provides a robust addition to the existing CMOS technology community.

Polycrystalline SnO thin films were deposited on *p*-type Si substrates (with a 106 nm-SiO_2 layer thermally grown on it) through electron-beam evaporation at room temperature (deposition details were reported elsewhere[19]), followed by rapid thermal annealing at 400 °C in Ar ambient (annealing details were reported elsewhere[15]). Figure 1(a) shows the x-ray diffraction (XRD) pattern in $\theta - 2\theta$ scans of the polycrystalline SnO film (JCPDS file No. 06-0395). It is found that the peaks in the XRD pattern can be well indexed to the litharge-type layered structure, as seen in the inset of Fig. 1(a). The x-ray photoelectron spectroscopy (XPS) measurement (Fig. 1(b)) depicts that a spin-orbit doublet peaked at $\sim$485.6 eV (Sn^{2+} $3d_{5/2}$) and $\sim$494.0 eV (Sn^{2+} $3d_{3/2}$) is

[a)]Author to whom correspondence should be addressed. Electronic mail: h_cao@nimte.ac.cn.

 © 2012 American Institute of Physics

Downloaded 26 Jun 2012 to 210.72.19.250. Redistribution subject to AIP license or copyright; see http://apl.aip.org/about/rights_and_permissions

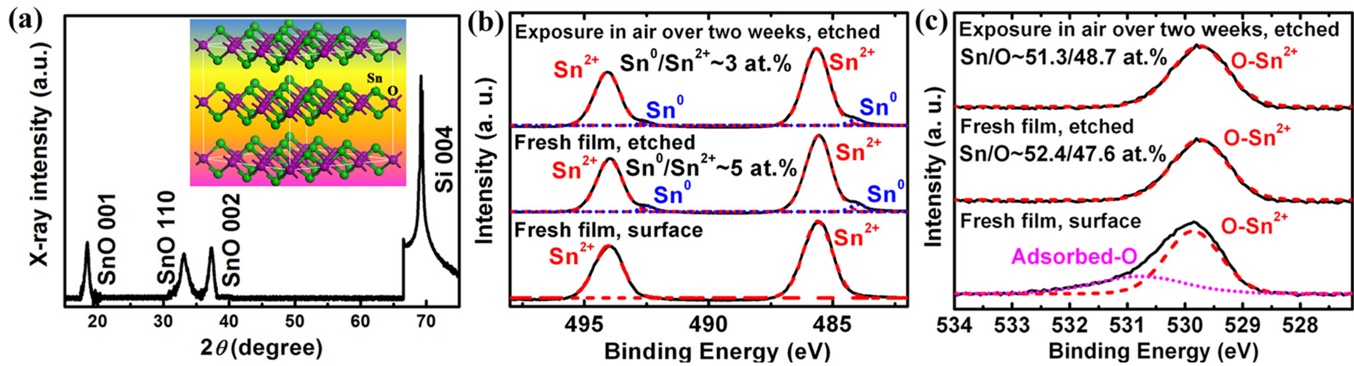

FIG. 1. (a) XRD patterns of polycrystalline SnO film on a Si substrate (with SiO_2 overcoat). The inset illustrates the crystal structure of SnO. (b) and (c) The Sn 3d and O 1s core level XPS spectra of the SnO films.

observed for the pristine film surface, while two small shoulders, centered at ~484.0 eV (Sn^0 $3d_{5/2}$) and ~492.5 eV (Sn^0 $3d_{3/2}$) are present for the etched sample (To obtain the chemical composition of the bulk layer of the SnO films, high doses of argon ions were utilized to sputter away the top layer of 3-4 nm.). The O 1s spectrum of the pristine film surface exhibits two peaks at ~529.8 eV and ~530.9 eV that could be assigned to O in SnO and adsorbed O on the outermost surface, respectively; while the O 1s spectra of the etched sample only present one peak corresponding to O in the SnO matrix (Fig. 1(c)). The Sn/O atomic ratio of the etched fresh sample was determined to be ~52.4/47.6, implying that the SnO films were a little oxygen deficient.

Shown in the inset of Fig. 2(a) is a schematic of a top-contact and bottom-gate (TC-BG) TFT with the polycrystalline SnO, Ni/Au (50/30 nm) and SiO_2 (106 nm) as the channel, source/drain electrode and gate dielectric, respectively. Ni/Au source and drain electrodes were electron-beam evaporated through shadow masks under high vacuum (10^{-4} Pa). All the device characteristics were measured at room temperature in air and in dark using a Keithley 4200 semiconductor parameter analyzer connected to a SÜSS PM5 probe station. In Fig. 2(a), the measured output characteristics exhibit a typical ambipolar feature that the type of accumulated carriers depends on the magnitude and polarity of gate (V_G) and drain (V_{DS}) voltages. A superposition of the standard saturated behavior for one carrier is observed at high gate voltage (V_G), while a superlinear (diode-like) current signature at low V_G and high V_{DS} due to injection of the opposite carrier. Figure 2(b) displays the V-shaped transfer curves of the SnO ambipolar TFTs under various V_{DS}. Near symmetric characteristics between *n*- and *p*-type operations were unambiguously observed. In addition, the carrier field-effect mobility was calculated using the standard equation of the metal–oxide–semiconductor field-effect transistors (MOSFETs). A saturation field-effect mobility (μ_{sat}) of ~0.16 $cm^2 V^{-1} s^{-1}$ and linear field-effect mobility (μ_{lin}) of ~0.32 $cm^2 V^{-1} s^{-1}$ for *p*-channel and ~0.63 $cm^2 V^{-1} s^{-1}$ (μ_{sat}) and ~1.02 $cm^2 V^{-1} s^{-1}$ (μ_{lin}) for *n*-channel operation were obtained, manifesting that the injection and transport of holes are comparable to those of the electrons. Such current-voltage characteristics of the ambipolar TFTs are believed to be caused by two key points as follows.

One of the challenges for constructing ambipolar transistors lies in the efficient and balanced injection of both carriers from the source/drain (S/D) electrodes into a single channel layer, depending on the selection of a channel with small band-gap and suitable band alignment between the S/D electrodes and semiconductor channel contact. The optimal charge injection takes place as the Fermi level of the source electrode lines up with the valence band maximum of the semiconductor for hole injection or as the Fermi level of the drain electrode matches with the conduction band minimum (CBM) for electron injection (V_{DS} is negative), and analogous source/CBM or drain/VBM band alignment is prerequisite to favor one carrier injection when V_{DS} is positive. SnO has a fundamental band-gap of ~0.5 eV, which reduces the technical difficulties to select S/D electrode materials and facilitates the band alignment matching to shrink the injection barriers. The commonly used Ni/Au or Au source-drain electrodes were utilized in this study to reduce injection barriers for both carriers. Figure 2(c) depicts a schematic band diagram of the SnO transistor at different V_G corresponding to the points highlighted in Fig. 2(b). At point A, the band bends significantly at the source, and the VBM of the SnO channel aligns with the source, consequently only holes can be injected effectively into the channel; while at point C, the band bends severely at the drain so that the CBM of the SnO channel aligns with the drain properly, resulting in that only electrons can be injected effectively into the channel. The injection barrier can be further decreased in a field-effect transistor, in which a lateral S/D electric field and a perpendicular gate field are applied simultaneously. At point B (where the gate voltage induces the minimum current, i.e., the onset voltage V_{on}), the potential of the transistor channel can be imagined as an equilibrium hole and electron channel in series, resulting in an s-shaped dividing line (see the band diagram). As observed in the typical ambipolar TFTs,[22,23] the onset voltages for the opposite carrier channel at whether negative or positive V_G shift with the applied V_{DS}, showing that V_{on} depends linearly on V_{DS} (Fig. 2(d)).

Another challenge is that the channel should have good conductivity for both carriers. It has been proposed that,[12,15] the VBM of SnO is mainly consisted of Sn 5s orbitals rather than localized O 2p ones, and the isotropic extended 5s orbitals contribute to form the sound hole transport paths. We carried out first-principles calculations to find out the CBM

Downloaded 26 Jun 2012 to 210.72.19.250. Redistribution subject to AIP license or copyright; see http://apl.aip.org/about/rights_and_permissions

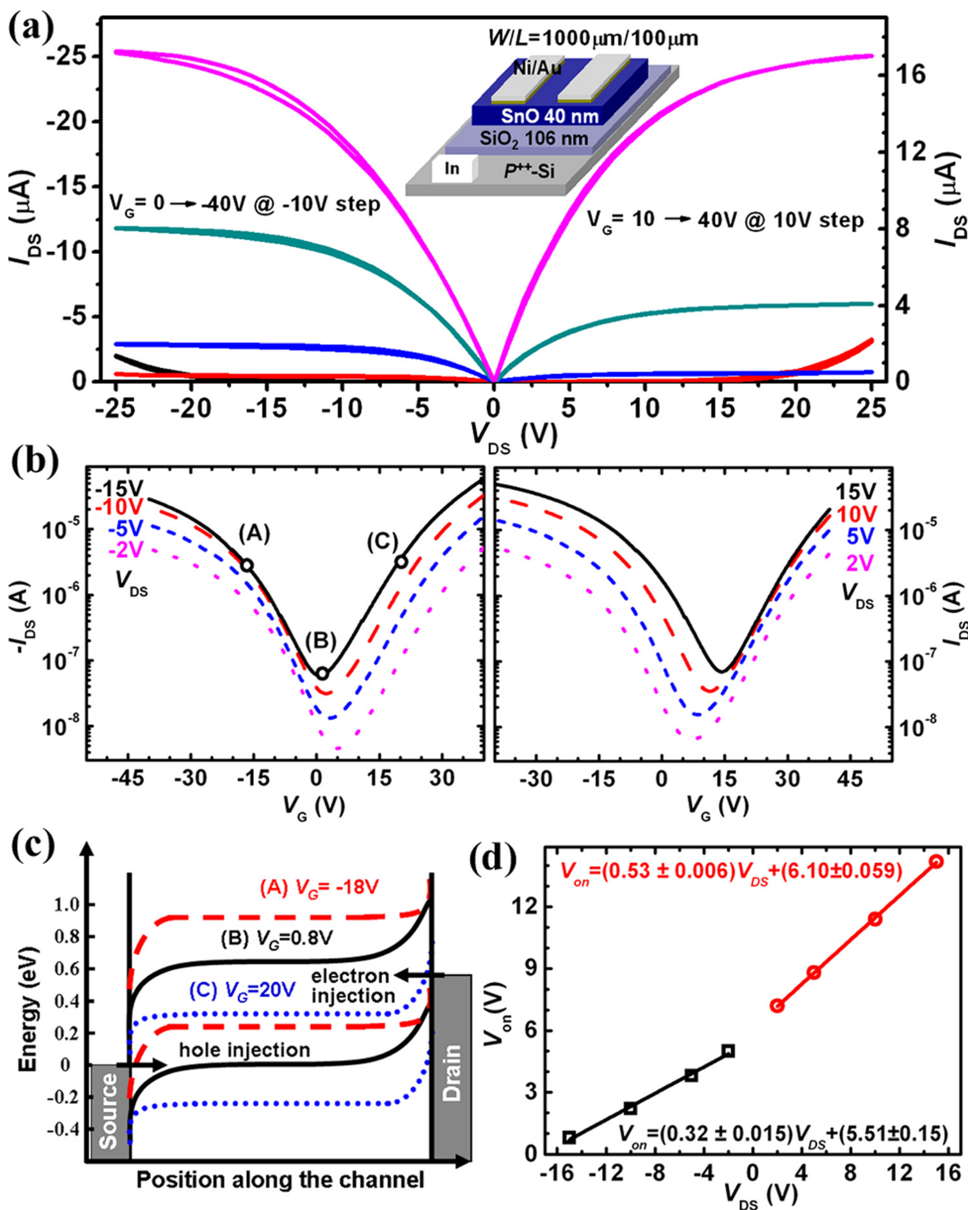

FIG. 2. (a) Output characteristics of the ambipolar SnO TFT under *p*-channel (left) and *n*-channel (right) operations. The inset shows the schematic diagram of the SnO TFTs. (b) Transfer characteristics of the same TFT at $V_{DS} < 0$ (left) and $V_{DS} > 0$ (right). Labeled points in the left figure are corresponding to the band diagrams shown in c. (c) Schematic band diagrams of the transistor at $V_G = -18$ V (red, dashed), 0.8 V (black, solid), and +20 V (blue, dotted), corresponding to the points labeled A, B, and C in b, respectively. (d) The linear dependence of V_{on} on V_{DS} at negative or positive V_{DS}.

structure of SnO, indicating that the CBM is mainly formed by the Sn 5p, as reported by Togo *et al.*[24] And interestingly, it is also revealed that the electron transport near the CBM follows the free-electron-like model very well, as described by $E = \hbar^2 k^2/2m_n$ (where E is the energy near the CBM, $\hbar$ the reduced Planck constant, k the wave vector, and m_n the effective mass of electrons). Therefore, SnO is capable of transporting both holes and electrons once the carriers are injected into it. Nomura *et al.* reported ambipolar TFTs using polycrystalline SnO as channels; the μ_{sat} in *n*-channel ($5 \times 10^{-4}\,\text{cm}^2\,\text{V}^{-1}\,\text{s}^{-1}$), however, was three orders of magnitude lower than that in *p*-channel.[21] They speculated that the ITO S/D electrodes blocked the electron injection. But nevertheless, the Fermi level of ITO lies above the VBM of SnO according to their experimental measurements, which would hinder the injection of holes rather than electrons. From the carrier transportation point of view, we believe that the oxygen-rich nature of the SnO channel could be the reason of the low electron mobility in their study. In fact, oxygen vacancies are known as the donors and excessive oxygen often kills free electrons in *n*-type metal oxide, while transition metal vacancies act as the acceptors which generate hole carriers in the *p*-type metal oxides.[25] This hypothesis is supported by the report of unipolar, *p*-channel TFTs using SnO_x films (with Sn^{2+} and Sn^{4+} coexisting) as channels.[18] Correspondingly, SnO channels with a little oxygen deficiency (Figs. 1(b) and 1(c)) might benefit the improvement of electron field-effect mobility, giving rise to balanced field-effect mobilities in *p*- and *n*- channel operations in this work.

The balanced ambipolar feature of SnO TFTs favors to construct CMOS-like inverters using two identical (the same geometry and dimension) transistors with a common gate as the input voltage V_{IN}. Shown in Figure 3(a) is the equivalent circuit diagram of the inverter, and such logic device configuration can reduce the patterning and fabricating processes to the minimum. The voltage transfer characteristics (VTCs) at different supply voltages (V_{DD}) are presented in Fig. 3(b), where the typical and comparable ambipolar inverter behaviors are seen in the first (positive V_{DD} and V_{IN}) and third quadrants (negative V_{DD} and V_{IN}). The extracted voltage

Downloaded 26 Jun 2012 to 210.72.19.250. Redistribution subject to AIP license or copyright; see http://apl.aip.org/about/rights_and_permissions

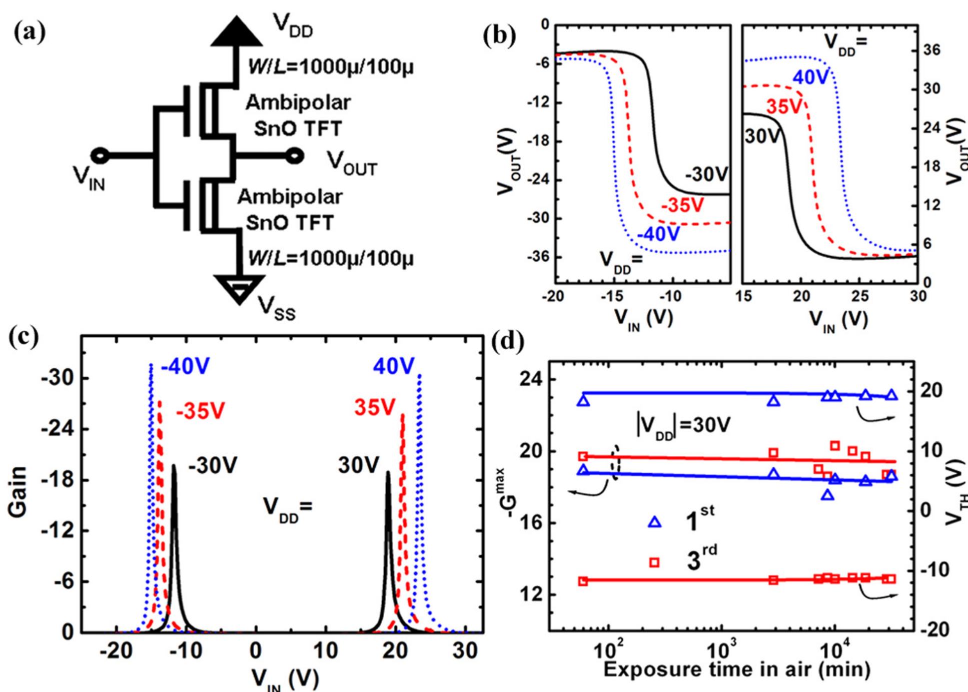

FIG. 3. (a) SnO ambipolar inverter circuit diagram. (b) VTCs of the CMOS-like inverter in the first (right) and third (left) quadrants, respectively. (c) Differential gain as a function of input voltage (V_{IN}). (d) Evolution of the maximum gain (G^{max}) and V_{TH} at $|V_{DD}| = 30$ V in the first and third quadrants as a function of exposure time to ambient air over a period of 3 weeks.

gain, defined as $\partial V_{OUT}/\partial V_{IN}$, is measured to be 30.6 ($V_{DD} = 40$ V) and 31.3 ($V_{DD} = -40$ V) in the first and third quadrants, respectively (Fig. 3(c)), which are comparable to those of the ambipolar inverters containing different channel materials such as microcrystalline silicon and organics.[21]

Another important advantage associated with our inverters is the superior air stability. The inverters were exposed to ambient air with a relative humidity in the range of 20%–30%, and then their characteristics were monitored as a function of exposure time. Figure 3(d) displays the maximum gain (G_{max}) and threshold voltage (V_{TH}) in the first and third quadrants over a period of several weeks. It can be seen that the inverter characteristics almost remain unaffected, which is probably attributed to the existence of Sn^0 preventing the oxidation of Sn^{2+} to Sn^{4+}, as shown in Fig. 1(b). This feature, combined with the circuit's high differential gain, good logic voltage swings (>82% of the highest output voltage), and wide noise margins (~20%), demonstrates that the SnO-based ambipolar inverter could be a robust building block of logic circuits for large area oxide electronics.[2,8]

In summary, ambipolar SnO transistors with balanced electron and hole field-effect mobilities were demonstrated experimentally by using a small band-gap semiconductor, electron-beam evaporated polycrystalline SnO as the single channel layer, and a common Ni/Au or Au as source/drain electrodes, respectively. CMOS-like inverters were constructed with the combination of two identical (both in geometry and dimension) ambipolar SnO-TFTs, featuring a maximum voltage gain as high as ~30. The devices are air stable, large area scalable, and easy to fabricate. This implementation would prompt the development of low-cost and large-area oxide-based integrated circuits.

This work is supported by the Chinese National Program on Key Basic Research Project (2012CB933003), the National Natural Science Foundation of China (Grant No. 11104289), the Science and Technology Innovative Research Team of Ningbo Municipality (2009B21005), the Key Program for Science and Technology Innovative Team of Zhejiang Province (2010R50020), and Applied Research Funds for Public Welfare Project of Zhejiang Provience (2011C21030).

[1]J. F. Wager, Science **300**, 1245 (2003).
[2]R. Martins, A. Nathan, R. Barros, L. Pereira, P. Barquinha, N. Correia, R. Costa, A. Ahnood, I. Ferreira, and E. Fortunato, Adv. Mater. **23**, 4491 (2011).
[3]K. Nomura, H. Ohta, A. Takagi, T. Kamiya, M. Hirano, and H. Hosono, Nature (London) **432**, 488 (2004).
[4]K. Nomura, H. Ohta, K. Ueda, T. Kamiya, M. Hirano, and H. Hosono, Science **300**, 1269 (2003).
[5]F. S. Kim, X. Guo, M. D. Watson, and S. A. Jenekhe, Adv. Mater. **22**, 478 (2010).
[6]K. Y. Chan, D. Knipp, J. Kirchhoff, A. Gordijn, and H. Stiebig, Solid-State Electron. **53**, 635 (2009).
[7]H. Hosono, Y. Ogo, H. Yanagi, and T. Kamiya, Electrochem. Solid-State Lett. **14**, H13 (2011).
[8]J. Smith, A. Bashir, G. Adamopoulos, J. E. Anthony, D. D. C. Bradley, R. Hamilton, M. Heeney, I. McCulloch, and T. D. Anthopoulos, Adv. Mater. **22**, 3598 (2010).
[9]H. Nakanotani, M. Yahiro, C. Adachi, and K. Yano, Appl. Phys. Lett. **90**, 262104 (2007).
[10]J. B. Kim, C. Fuentes-Hernandez, S.-J. Kim, S. Choi, and S. B. Kippelen, Org. Electron. **11**, 1074 (2010).
[11]W. Guo, L. Fu, Y. Zhang, K. Zhang, G. Graham, L. Y. Liang, Z. M. Liu, H. T. Cao, and X. Q. Pan, Appl. Phys. Lett. **96**, 042113 (2010).
[12]Y. Ogo, H. Hiramatsu, K. Nomura, H. Yanagi, T. Kamiya, M. Hirano, and H. Hosono, Phys. Status Solidi A **206**, 2187 (2009).
[13]Y. Ogo, H. Hiramatsu, K. Nomura, H. Yanagi, T. Kamiya, M. Hirano, and H. Hosono, Appl. Phys. Lett. **93**, 032113 (2008).
[14]L. Y. Liang, Z. M. Liu, H. T. Cao, W. Y. Xu, X. L. Sun, H. Luo, and K. Cang, J. Phys. D: Appl. Phys. **45**, 085101 (2012).
[15]L. Y. Liang, Z. M. Liu, H. T. Cao, Z. Yu, Y. Y. Shi, A. H. Chen, H. Z. Zhang, Y. Q. Fang, and X. L. Sun, J. Electrochem. Soc. **157**, H598 (2010).
[16]E. Fortunato, R. Barros, P. Barquinha, V. Figueiredo, S. H. K. Park, E. Elamurugu, C. S. Hwang, and R. Martins, Appl. Phys. Lett. **97**, 052105 (2010).
[17]H. Yabuta, N. Kaji, R. Hayashi, H. Kumomi, K. Nomura, T. Kamiya, M. Hirano, and H. Hosono, Appl. Phys. Lett. **97**, 072111 (2010).
[18]C. W. Ou, Dhananjay, Z. Y. Ho, Y. C. Chuang, S. S. Cheng, M. C. Wu, K. C. Ho, and C. W. Chu, Appl. Phys. Lett. **92**, 122113 (2008).

Downloaded 26 Jun 2012 to 210.72.19.250. Redistribution subject to AIP license or copyright; see http://apl.aip.org/about/rights_and_permissions

[19]L. Y. Liang, Z. M. Liu, H. T. Cao, Y. Y. Shi, X. L. Sun, Z. Yu, A. H. Chen, H. Z. Zhang, and Y. Q. Fang, ACS Appl. Mater. Interfaces **2**, 1565 (2010).
[20]E. J. Meijer, D. M. Leeuw, E. V. Veenendaal, S. Setayesh, B. H. Huisman, P. W. M. Blom, J. C. Hummelen, U. Scherf, and T. M. Klapwijk, Nature Mater. **2**, 678 (2003).
[21]K. Nomura, T. Kamiya, and H. Hosono, Adv. Mater. **23**, 343 (2011).
[22]J. Zaumseil and H. Sirringhaus, Chem. Rev. **107**, 1296 (2007).
[23]M. Radosavljevic, S. Heinze, J. Tersoff, and Ph. Avouris, Appl. Phys. Lett. **83**, 2435 (2003).
[24]A. Togo, F. Oba, and I. Tanaka, Phys. Rev. B **74**, 195128 (2006).
[25]S. Lany, J. Osorio-Guillén, and A. Zunger, Phys. Rev. B **75**, 241203 (2007).

Downloaded 26 Jun 2012 to 210.72.19.250. Redistribution subject to AIP license or copyright; see http://apl.aip.org/about/rights_and_permissions